Journal of Mathematical Modeling
Vol. 14, No. 2, 2026, pp. 407-430. Research Article

JMM

Modeling and analysis of deforestation and pollution dynamics induced by industrialization using the fractal-fractional Atangana-Baleanu derivative

Nobin Daimary*, Ranu Paul

Department of Mathematics, Gauhati University, Guwahati-14, Assam, India

Email(s): nobindaimary12@gmail.com, ranupaul1984@gauhati.ac.in

Abstract. This study presents a fractal-fractional model in the Atangana–Baleanu sense to investigate the dynamics of deforestation and pollution driven by industrialization. The model is analyzed for positivity and boundedness, and the existence and uniqueness of its solution are established using fixed-point theory. The system's equilibrium points are identified, and the threshold parameter $\mathfrak{R}_o$ is determined, with local asymptotic stability confirmed for all equilibria. Sensitivity analysis highlights the key parameters influencing $\mathfrak{R}_o$, while Ulam–Hyers stability ensures robustness of the solution. Lagrangian polynomial interpolation is employed to approximate the solution, and phase portraits along with numerical simulations in Matlab illustrate the model's dynamic behavior. The results demonstrate that the fractal-fractional approach provides a comprehensive framework for capturing complex environmental interactions, offering valuable insights into the effects of industrialization on deforestation and pollution.

Keywords: Atangana-Baleanu fractal–fractional operator, stability, Ulam-Hyres stability.
AMS Subject Classification 2020: 26A33, 65M99, 28A80.

1 Introduction

Deforestation due to industrialization represents a critical environmental challenge, characterized by the systematic clearing of forested areas to facilitate industrial growth and economic development. Driven by increasing demands for resources, space, and improved living standards, industrial expansion often entails logging for timber, land clearance for manufacturing plants, the construction of transportation infrastructure, and the extraction of natural resources such as minerals and fossil fuels. While industrialization fosters economic progress, it simultaneously engenders profound environmental consequences,

*Corresponding author
Received: 15 August 2025/ Revised: 28 October 2025/ Accepted: 6 November 2025
DOI: 10.22124/jmm.2025.31414.2822

including biodiversity loss, habitat destruction, and the exacerbation of climate change through reduced carbon dioxide (CO_2) absorption. Additionally, deforestation contributes to soil erosion, disrupts hydrological cycles, and adversely affects indigenous communities dependent on forest ecosystems. Industrialization also introduces significant pollution into the environment, as emissions from factories, power plants, and other facilities release harmful gases and particulates-such as sulphur dioxide (SO_2), nitrogen oxides (NO_x), carbon monoxide (CO), and volatile organic compounds ($VOCs$)-which contribute to air quality degradation, smog formation, acid rain, and respiratory illnesses. Furthermore, greenhouse gas emissions from industrial activities are major drivers of global warming. Prior to industrialization, atmospheric CO_2 levels were relatively low; however, the end of the last ice age and the advent of the Industrial Revolution led to substantial increases [30]. Water pollution results from the discharge of untreated or inadequately treated industrial waste containing toxic chemicals and heavy metals into aquatic ecosystems, while soil pollution arises from the improper disposal of industrial waste and the use of hazardous substances, leading to the deterioration of soil quality and agricultural productivity. In response to these environmental impacts, afforestation is the planting of trees in previously non-forested areas-serves as a crucial mitigation strategy. By restoring lost forests and enhancing green cover, afforestation helps to improve air quality, sequester carbon, purify water, remediate soils, and restore ecosystems, offering a natural and effective solution to the dual challenges of deforestation and pollution caused by industrialization.

Over the past few decades, numerous studies have employed integer-order mathematical models to investigate the effects of population growth and industrialization on the depletion of biomass resources. For instance, Shukla et al. [22] developed a dynamic model to analyze the impact of industrialization on biomass resource degradation. Shukla and Dubey [21] have developed and examined a mathematical model to investigate how pollution and population growth affect resource biomass when contaminants are released into the ecosystem at steady rates from outside sources. In [17], the authors have proposed and analyzed a mathematical model to study the depletion of forestry resources caused simultaneously by population growth and population pressure augmented by industrialization. Dubey and Dass [7] have developed and examined a mathematical model that takes into account the effects of species diffusion in order to investigate the survival of species that are dependent on a resource that is being depleted as a result of industrialization. In [11], the authors investigated the impact of mining activities and pollution on forest resources and wildlife populations using a mathematical model.

In recent years, fractional differential equations (FDEs) have gained significant attention across various scientific and engineering fields due to their ability to yield more accurate and realistic results. The non-local nature of fractional derivatives makes them particularly effective for capturing the memory effects inherent in complex physical systems. In the past few decades, several fractional operators with distinct kernels have been introduced. Notably, the Caputo operator [18] features a singular kernel, while the Caputo–Fabrizio [5] and Atangana–Baleanu [2] operators employ non-singular kernels. These operators are associated with different underlying behaviors, including power laws, exponential decay laws, and generalized Mittag-Leffler functions. For instance, approximate analytical solutions to the Bagley–Torvik equation were obtained using the fractional iteration method, demonstrating the versatility of fractional calculus in handling systems that exhibit both viscous and elastic behavior [16]. A Caputo–Fabrizio fractional model has been proposed to study HIV/AIDS dynamics, focusing on individuals unaware of their infection. The study analyzes stability using the abdicate method and linear matrix inequalities (LMI), and employs optimal control to identify effective intervention strategies [15]. Karthikeyan et al. [12] analyzed a fractional-order predator–prey model that includes prey refuge and

predator anti-predator behavior. Fractional operators have expanded to nonlinear and spatio-temporal systems, with the beta-derivative effectively modeling traveling waves in nonlinear directional couplers [24]. Verma et al. proposed a combined SIR–SI fractional-order model for dengue transmission, incorporating memory effects through Caputo derivatives [29]. Additionally, they introduced a fuzzy fractional model of the human liver using ABC gH-differentiability based on the generalized Hukuhara derivative, and applied a fuzzy double parametric q-homotopy analysis method with a generalized transform to study the model and its convergence [28]. Fahimi et al. [9] developed a new mathematical model describing the spread of epidemic diseases with vaccination, focusing on Chinese measles. Singh et al. [23] proposed a new approach for solving a time-fractional cancer tumor model using Caputo, CF, and ABC derivatives, considering variable net-killing rates in an uncertain environment.

Atangana Abdon [1] introduced the fractal–fractional (FF) derivative, a novel operator that integrates power-law, exponential, and generalized Mittag-Leffler behaviors with fractal derivatives, including variants such as the fractal–fractional Caputo derivative, fractal–fractional Caputo–Fabrizio derivative, and fractal–fractional Atangana–Baleanu derivative. This operator combines fractional calculus and fractal theory, capturing both memory effects and complex geometric structures. The fractional component accounts for historical dependence, while the fractal component models self-similar, irregular patterns in non-integer dimensions. In environmental contexts, it can describe phenomena such as pollution accumulation, ecological degradation, and forest dynamics, where past events influence future outcomes in fractal-like spatial patterns. Due to the exceptional accuracy of these operators in numerically simulating solutions for various FF systems, numerous researchers have developed several FF models. Gomez-Aguilar et al. used FF derivatives to study a malaria transmission model [10]. The researchers in [20] examined the SARS-CoV-2 outbreak in Pakistan through the application of FF derivatives. Awadalla et al. explored the impact of fractal-fractional operators in the mathematical modeling of corruption [4]. In [19], M. Rahman analyzed the FF mathematical problem of an Atangana-Baleanu in the sense of the Caputo fractional operator with a non-singular Mittag-Leffler kernel. An analysis of a Mittag-Leffler FF derivative TB and HIV co-infection model was conducted in [14]. D. Baleanu et al. investigated a FF model of the AH1N1/09 virus via power law-type kernels in [8]. An FF waterborne disease model was studied in [13]. Verma et al. [27] developed a temporal fractional HIV/AIDS model incorporating fractal dimensions to analyze the impact of awareness on disease dynamics using Indian data from 1990–2016.

The primary objective of this study is to develop and analyze a mathematical model that captures the dynamics of deforestation and pollution driven by industrialization, incorporating both memory effects and fractal geometries using the Atangana-Baleanu fractal-fractional derivative.

The accelerating pace of industrialization across the globe has intensified the pressures on forest ecosystems and exacerbated environmental pollution, threatening biodiversity, human health, and climate stability. Traditional integer-order models often fail to capture the long-term memory effects and complex, self-similar patterns inherent in ecological and industrial systems. Fractal-fractional calculus, particularly in the Atangana-Baleanu sense, offers a novel framework to model these phenomena by simultaneously accounting for historical dependencies and fractal structures, providing a more realistic representation of deforestation, afforestation, industrial growth, and pollution dynamics. Despite growing interest in fractional and fractal-fractional modeling in biological and epidemiological contexts, their application to environmental systems impacted by industrialization remains limited. The present research is motivated by the urgent need to develop mathematically rigorous models that integrate memory effects and fractal geometries to better understand the nonlinear interactions between industrial activities, deforestation, afforestation, and pollution,offering insights for sustainable mitigation strategies.

The present article is organized as follows. In Section 2, the definitions of FF operators based on the Mittag-Lefler type kernel and some important theorems that are required for the next sections are provided. Section 3 presents the mathematical formulation of the proposed model using integer-order derivatives. In Section 4, the positivity and boundedness of the solution of the integer order model are studied. The equilibrium points of the model are determined in Section 5. The local stability of the equilibrium points are investigated in Section 6. In Section 7, the proposed model is generalized to a fractal–fractional form in the sense of the Atangana–Baleanu derivative. Section 8 discusses the existence and uniqueness of the model solutions under the fractal–fractional derivative framework. In Section 9, the Ulam-Hyers stability is discussed. The sensitivity analysis is presented in Section 10. Sections 11 and 12 illustrate the numerical method and the numerical simulations, respectively. In Section 13, we end the paper with our conclusions.

2 Preliminaries

In this section, we state the definitions of fractal-fractional derivative and integral operators based on the generalized Mittag-Leffler type kernel and some concepts that are required in the next sections.

Definition 1 ([3]). *Suppose that $y(t)$ is a continuous and fractal-differentiable function of order τ on the interval (a,b). Then, the* fractal-fractional derivative *of $y(t)$ of order α, in the* Liouville–Caputo sense *with a* generalized Mittag-Leffler type kernel*, is defined as:*

$$ {}^{FF-ABC}D_{0,t}^{\alpha,\tau}(y(t)) = \frac{ABC(\alpha)}{1-\alpha}\int_0^t E_\alpha\Big(-\frac{\alpha}{1-\alpha}(t-s)^\alpha\Big)\frac{dy(s)}{ds^\tau}\,ds, \tag{1} $$

where $E_\alpha(.)$ denotes the Mittag-Leffler function, $0<\alpha,\tau\le 1$, $\frac{dy(s)}{ds^\tau} = \lim_{t\to s}\frac{y(t)-y(s)}{t^\tau-s^\tau}$ and $ABC(\alpha) = 1-\alpha+\frac{\alpha}{\Gamma(\alpha)}$.

Definition 2 ([3]). *Suppose that $y(t)$ be continuous on an open interval (a,b), then the fractal-fractional integral of $y(t)$ with order α having Generalized Mittag-Leffler type kernel is defined as follows:*

$$ {}^{FF-ABC}J_{0,t}^{\alpha,\tau}(y(t)) = \frac{\alpha\tau}{ABC(\alpha)}\int_0^t s^{\tau-1}(t-s)^{\alpha-1}y(s)\,ds + \frac{\tau(1-\alpha)t^{\tau-1}y(t)}{ABC(\alpha)}. \tag{2} $$

Lemma 1 ([4]). *A solution for the problem*

$$ {}^{FF-ABC}D_{0,t}^{\alpha,\tau}(y(t)) = \tau t^{\tau-1}\mathbb{F}(t,y(t)),\ \ t\in[0,T], $$
$$ y(0) = y_0,\ 0<\alpha,\tau\le 1, $$

is provided by

$$ y(t) = y_0 + \frac{1-\alpha}{ABC(\alpha)}t^{\tau-1}\mathbb{F}(t,y(t)) + \frac{\alpha\tau}{ABC(\alpha)\Gamma(\alpha)}\int_0^t \lambda^{\tau-1}(t-\lambda)^{\alpha-1}\mathbb{F}(\lambda,y(\lambda))\,d\lambda. $$

Table 1: The parameter descriptions of the model

Parameter	Description
r	Intrinsic growth rate of industrialization.
K	Carrying capacity or maximum potential for industrialization.
β	Rate of depletion of industrialization due to afforestation.
μ_1	Control rate of industrialization applied by government agencies.
θ	Rate at which deforestation increases due to industrialization.
μ_2	Rate at which deforestation reduces due to afforestation efforts.
A_0	Constant growth rate of afforestation.
μ_3	Natural depletion rate of afforestation.
P_0	Constant growth rate of pollution due to pollutants emitted from different sources.
δ	Growth rate of pollution due to industrialization and deforestation.
γ	Depletion rate of pollution due to afforestation.
μ_4	Natural depletion rate of pollution.

3 Model formulation

At any time t, we consider four dynamical variables: the level of industrialization (denoted by $I(t)$), the level of deforestation (denoted by $D(t)$), the level of afforestation (denoted by $A(t)$), and the level of pollution (denoted by $P(t)$). We assume that industrialization grows logistically and is controlled by government authorities. Also, it decreases due to afforestation. Here, we assume that the growth of deforestation is directly proportional to the level of industrialization. The growth rate of afforestation is supposed to be constant. The growth rate of pollution level emitted from different sources is assumed to be constant. However, it is also assumed that the level of pollution increases due to industrialization. Based on these assumptions, we construct an integer-order mathematical model with variables I, D, A, and P as follows:

$$\begin{aligned}
\frac{dI(t)}{dt} &= rI(t)\left(1-\frac{I(t)}{K}\right)-\beta A(t)I(t)-\mu_1 I(t),\\
\frac{dD(t)}{dt} &= \theta I(t)-\mu_2 A(t)D(t),\\
\frac{dA(t)}{dt} &= A_0-\mu_3 A(t),\\
\frac{dP(t)}{dt} &= P_0+\delta I(t)D(t)-\gamma A(t)P(t)-\mu_4 P(t),
\end{aligned} \tag{3}$$

with the initial conditions

$$I(0)\geq 0, D(0)\geq 0, A(0)\geq 0, P(0)\geq 0.$$

All parameters are assumed to be positive, which are listed in Table 1.

4 Positivity and boundedness

We investigate the positivity and boundedness properties of the solutions to the integer-order system (3) in this section.

Theorem 1. *Any solution of the system with initial condition* $(I(t_0),D(t_0),A(t_0),P(t_0)) \in \mathbb{R}^4_+$ *remains non-negative for all* $t \geq t_0$.

Proof. Let $X(t_0) = (I(t_0),D(t_0),A(t_0),P(t_0)) \in \Gamma^+ = \{(I,D,A,P) \in \Gamma^+ : I,D,A,P \in \mathscr{R}^+\}$ be the initial point of solution of the model.

Let us consider that there exists a constant t_1, $t_0 \leq t < t_1$ such that

$$\begin{aligned} &A(t) > 0, \;\; t_0 \leq t < t_1, \\ &A(t_1) = 0, \\ &A(t_1^+) < 0. \end{aligned}$$

By analyzing the third equation of system(3), we obtain

$$\left|\frac{dA}{dt}\right|_{A(t)=0} = A_0 \geq 0.$$

It follows that at any time the solution reaches the axis, its derivative increases, and so the function $A(t)$ is non-decreasing, i.e. $A(t_1^+) \geq 0$ which contradicts our assumption that $A(t_1^+) < 0$. Therefore, we get $A(t) \geq 0, \forall t \in [t_0,\infty)$. Similarly, we can show that $I(t) \geq 0, D(t) \geq 0, P(t) \geq 0, \forall t \in [t_0,\infty)$. Thus, for any positive initial conditions, all the solutions are positive. □

Theorem 2. *The region given by* $\Omega \in \mathbb{R}^4_+$ *such that* $\Omega = \left\{(I,D,A,P) \in \mathbb{R}^4_+ : 0 < I \leq K,\ 0 < D \leq \frac{\theta K \mu_3}{\mu_2 A_0},\ 0 < A \leq \frac{A_0}{\mu_3},\ 0 < P \leq \frac{\mu_3(\mu_2 A_0 P_0 + \delta\theta\mu_3 K^2)}{\mu_2 A_0(\gamma A_0 + \mu_3\mu_4)}\right\}$ *is bounded and positively invariant for the system with the initial conditions in* $\mathbb{R}^4_+$.

Proof. Using the comparison theorem of differential equations, from the first equation of model (3), we get

$$\frac{dI}{dt} \leq rI\left(1 - \frac{I}{K}\right).$$

Integrating using the separation of variables method, we get the solution as

$$\begin{aligned} I(t) &= \frac{K}{1 + Be^{-rt}}, \\ \lim_{t\to\infty} I(t) &\to K, \end{aligned}$$

where B is a constant.
From the third equation of system (3), we get

$$\frac{dA}{dt} = A_0 - \mu_3 A,$$

$$\frac{dA}{dt} + \mu_3 A = A_0.$$

The integrating factor is $e^{\int \mu_3 \, dt} = e^{\mu_3 t}$, thus the solution is

$$\begin{aligned} Ae^{\mu_3 t} &= \int A_0 e^{\mu_3 t} \, dt + C = \frac{A_0}{\mu_3} e^{\mu_3 t} + C, \\ A(t) &= \frac{A_0}{\mu_3} + Ce^{-\mu_3 t}, \end{aligned}$$

where C is a constant. Using initial condition $A(0)$, we get

$$C = A(0) - \frac{A_0}{\mu_3}.$$

Thus, we get

$$\begin{aligned} A(t) &= \frac{A_0}{\mu_3} + \left(A(0) - \frac{A_0}{\mu_3}\right) e^{-\mu_3 t}, \\ &= \frac{A_0}{\mu_3}(1 - e^{-\mu_3 t}) + A(0)e^{-\mu_3 t}, \\ \lim_{t \to \infty} A(t) &\to \frac{A_0}{\mu_3}. \end{aligned}$$

Furthermore, by considering the second equation of the model, we obtain

$$\begin{aligned} \frac{dD}{dt} &= \theta K - \mu_2 \frac{A_0}{\mu_3} D, \\ \frac{dD}{dt} &+ \frac{\mu_2 A_0}{\mu_3} D = \theta K. \end{aligned}$$

Applying the same procedure as discussed above, we get

$$\begin{aligned} D(t) &= \frac{\theta K \mu_3}{\mu_2 A_0}(1 - e^{-\frac{\mu_2 A_0}{\mu_3} t}) + D(0)e^{-\frac{\mu_2 A_0}{\mu_3} t}, \\ \lim_{t \to \infty} D(t) &\to \frac{\theta K \mu_3}{\mu_2 A_0}. \end{aligned}$$

In a similar manner, the final equation of the system yields

$$\begin{aligned} \frac{dP}{dt} &= P_0 + \delta ID - \gamma AP - \mu_4 P, \\ \frac{dP}{dt} &= P_0 + \delta K \frac{\theta K \mu_3}{\mu_2 A_0} - \left(\gamma \frac{A_0}{\mu_3} + \mu_4\right) P, \\ \frac{dP}{dt} &+ \frac{\gamma A_0 + \mu_3 \mu_4}{\mu_3} P = \frac{\mu_2 A_0 P_0 + \delta \theta \mu_3 K^2}{\mu_2 A_0}. \end{aligned}$$

So, we get

$$P(t) = \frac{\mu_2 A_0 P_0 + \delta\theta\mu_3 K^2}{\mu_2 A_0} \frac{\mu_3}{\gamma A_0 + \mu_3\mu_4} \left(1 - e^{-\frac{\gamma A_0 + \mu_3\mu_4}{\mu_3} t}\right) + P(0) e^{-\frac{\gamma A_0 + \mu_3\mu_4}{\mu_3} t},$$

$$\lim_{t\to\infty} P(t) \to \frac{\mu_3(\mu_2 A_0 P_0 + \delta\theta\mu_3 K^2)}{\mu_2 A_0(\gamma A_0 + \mu_3\mu_4)}. \qquad \square$$

5 Equilibrium points

In this section, we obtain the possible equilibrium points of system (3). The proposed model possess two equilibrium points, $E^0 = (0, \frac{A_0}{\mu_3}, 0, \frac{\mu_3 P_0}{\mu_3\mu_4 + \gamma A_0})$ and the coexisting equilibrium point $E^* = (I^*, D^*, A^*, P^*)$. These two equilibrium points can be obtained by solving the following system of nonlinear equations:

$$\begin{aligned} &rI(1 - \frac{I}{K}) - \beta AI - \mu_1 I = 0, \\ &\theta I - \mu_2 AD = 0, \\ &A_0 - \mu_3 A = 0, \\ &P_0 + \delta ID - \gamma AP - \mu_4 P = 0. \end{aligned} \tag{4}$$

The second and third equations of system (4) yeild

$$D = \frac{\theta\mu_3}{\mu_2 A_0} I,$$
$$A = \frac{A_0}{\mu_3}.$$

It follows from the first equation of system (4) that

$$I\left(r(1 - \frac{I}{K}) - \beta A - \mu_1\right) = 0, \text{ which implies either } I = 0, \text{ or } I = \frac{K[r\mu_3 - (\beta A_0 + \mu_1\mu_3)]}{r\mu_3}.$$

If $I = 0$, then $D = 0$, $A = \frac{A_0}{\mu_3}$, $P = \frac{\mu_3 P_0}{\mu_3\mu_4 + \gamma A_0}$. Again, if $I = \frac{K[r\mu_3 - (\beta A_0 + \mu_1\mu_3)]}{r\mu_3}$, then

$$P = \frac{\mu_3[r\mu_2 A_0 P_0 + \theta\delta K\{r\mu_3 - (\beta A_0 + \mu_1\mu_3)\}I]}{r\mu_2 A_0(\gamma A_0 + \mu_3\mu_4)}.$$

Thus $E^* = (I^*, D^*, A^*, P^*)$, where

$$\begin{aligned} I^* &= \frac{K[r\mu_3 - (\beta A_0 + \mu_1\mu_3)]}{r\mu_3}, \\ &= \frac{K(\beta A_0 + \mu_1\mu_3)(\mathfrak{R}_o - 1)}{r\mu_3}, \\ D^* &= \frac{\theta\mu_3}{\mu_2 A_0} I^*, \\ A^* &= \frac{A_0}{\mu_3}, \end{aligned}$$

$$P^* = \frac{\mu_3[r\mu_2 A_0 P_0 + \theta\delta K\{r\mu_3 - (\beta A_0 + \mu_1\mu_3)\}I^*]}{r\mu_2 A_0(\gamma A_0 + \mu_3\mu_4)},$$
$$= \frac{\mu_3[r\mu_2 A_0 P_0 + \theta\delta K(\beta A_0 + \mu_1\mu_3)(\Re_o - 1)I^*]}{r\mu_2 A_0(\gamma A_0 + \mu_3\mu_4)}.$$

It will exist only when $r\mu_3 - (\beta A_0 + \mu_1\mu_3) > 0$. We define a threshold quantity $\Re_o = \frac{r\mu_3}{(\beta A_0 + \mu_1\mu_3)}$. So, E^* exists only if $\Re_o > 1$.

6 Local stability of system

The following matrix represents the Jacobian of model (3) at (I, D, A, P) :

$$J = \begin{pmatrix} r - \frac{2rI}{K} - \beta A - \mu_1 & 0 & -\beta I & 0 \\ \theta & -\mu_2 A & -\mu_2 D & 0 \\ 0 & 0 & -\mu_3 & 0 \\ \delta D & \delta I & -\gamma P & -\gamma A - \mu_4 \end{pmatrix}.$$

The equilibrium points of system (3) are asymptotically stable if and only if all of the eigenvalues of the associated Jacobian matrix have the negative real parts.

Theorem 3. *The equilibrium point* $E^0 = (0, \frac{A_0}{\mu_3}, 0, \frac{\mu_3 P_0}{\mu_3\mu_4 + \gamma A_0})$ *is locally asymptotically stable if* $\Re_o < 1$ *and unstable otherwise.*

Proof. The Jacobian matrix of system (3) at the equilibrium point E^0 is

$$J(E^0) = \begin{pmatrix} r - \beta\frac{A_0}{\mu_3} - \mu_1 & 0 & 0 & 0 \\ \theta & -\mu_2\frac{A_0}{\mu_3} & 0 & 0 \\ 0 & 0 & -\mu_3 & 0 \\ 0 & 0 & -\gamma\frac{\mu_3 P_0}{\mu_3\mu_4 + \gamma A_0} & -\gamma\frac{A_0}{\mu_3} - \mu_4 \end{pmatrix}.$$

The characteristic equation of the above matrix is

$$\left(r - \beta\frac{A_0}{\mu_3} - \mu_1 - \lambda\right)\left(-\mu_2\frac{A_0}{\mu_3} - \lambda\right)(-\mu_3 - \lambda)\left(\gamma\frac{A_0}{\mu_3} - \mu_4 - \lambda\right) = 0,$$

which gives

$$\lambda_1 = r - \beta\frac{A_0}{\mu_3} - \mu_1 = \frac{(\beta A_0 + \mu_1\mu_3)(\Re_o - 1)}{\mu_3},$$
$$\lambda_2 = -\mu_2\frac{A_0}{\mu_3} < 0,$$
$$\lambda_3 = -\mu_3 < 0,$$
$$\lambda_4 = -(\gamma\frac{A_0}{\mu_3} + \mu_4) < 0.$$

We deduce that all the eigenvalues have negative real parts except λ_1. Also, λ_1 is negative if $\Re_o < 1$. Hence, E^0 is locally asymptotically stable if $\Re_o < 1$. Furthermore, if $\Re_o > 1$ then it is unstable. □

Theorem 4. *The coexisting equilibrium point $E^* = (I^*, D^*, A^*, P^*)$ is locally asymptotically stable when $\Re_o > 1$.*

Proof. The Jacobian matrix of system (3) at the positive equilibrium E^* is

$$J = \begin{pmatrix} r - \frac{2rI^*}{K} - \beta A^* - \mu_1 & 0 & -\beta I^* & 0 \\ \theta & -\mu_2 A^* & -\mu_2 D^* & 0 \\ 0 & 0 & -\mu_3 & 0 \\ \delta D^* & \delta I^* & -\gamma P^* & -\gamma A^* - \mu_4 \end{pmatrix}.$$

The two eigenvalues are

$$\lambda_1 = -\mu_2 A^* = -\mu_2 \frac{A_0}{\mu_3},\ \lambda_2 = -\mu_3.$$

The other two Eigenvalues can be found by solving the following characteristic equation:

$$(\gamma A^* - \mu_4 - \lambda)\left(r - \frac{2rI^*}{K} - \beta A^* - \mu_1 - \lambda\right) = 0.$$

Then

$$\begin{aligned}
\lambda_3 &= -\gamma A^* - \mu_4 = -(\gamma \frac{A_0}{\mu_3} + \mu_4), \\
\lambda_4 &= r - \frac{2rI^*}{K} - \beta A^* - \mu_1, \\
&= r - \beta \frac{A_0}{\mu_3} - \mu_1 - \frac{2rK(\beta A_0 + \mu_1\mu_3)(\Re_o - 1)}{Kr\mu_3}, \\
&= \frac{r\mu_3 - (\beta A_0 + \mu_1\mu_3) - 2(\beta A_0 + \mu_1\mu_3)(\Re_o - 1)}{\mu_3}, \\
&= \frac{(\beta A_0 + \mu_1\mu_3)(\Re_o - 1) - 2(\beta A_0 + \mu_1\mu_3)(\Re_o - 1)}{\mu_3}, \\
&= \frac{-(\beta A_0 + \mu_1\mu_3)(\Re_o - 1)}{\mu_3}.
\end{aligned}$$

We conclude that all the eigenvalues have negative real parts except λ_4. Also, λ_4 will be negative if $\Re_o > 1$. Therefore, E^* is locally asymptotically stable if $\Re_o > 1$. □

7 Fractal-fractional model

In this section, model (3) is generalized to a FF form based on the Atangana–Baleanu (AB) derivative. The resulting system is represented as follows:

$$\begin{aligned}
{}^{FF-ABC}D_{0,t}^{\alpha,\tau} I(t) &= rI(t)\left(1 - \frac{I(t)}{K}\right) - \beta A(t)I(t) - \mu_1 I(t), \\
{}^{FF-ABC}D_{0,t}^{\alpha,\tau} D(t) &= \theta I(t) - \mu_2 A(t)D(t),
\end{aligned} \tag{5}$$

$$
\begin{aligned}
{}^{FF-ABC}D_{0,t}^{\alpha,\tau} A(t) &= A_0 - \mu_3 A(t),\\
{}^{FF-ABC}D_{0,t}^{\alpha,\tau} P(t) &= P_0 + \delta I(t) D(t) - \gamma A(t) P(t) - \mu_4 P(t),
\end{aligned}
$$

where, ${}^{FF-ABC}D_{0,t}^{\alpha,\tau}(.)$ represents the fractal-fractional derivative of order $0 < \alpha \leq 1$ and fractal order $0 < \tau \leq 1$, defined in the sense of the Atangana-Baleanu operator with a generalized Mittag-Leffler kernel, subject to the following initial conditions:

$$I(0) \geq 0, D(0) \geq 0, A(0) \geq 0, P(0) \geq 0.$$

8 Existence and uniqueness

This section presents an analysis of the existence and uniqueness of the solution to system (5) based on the Picard–Lindel of theorem.

Consider the Banach space $\mathbb{U} = X^4$, where $X = C(0,T)$ under the norm

$$\|\mathbf{M}\|_X = \|(I(t), D(t), A(t), P(t))\|_X = max\{\Re(t) : t \in [0,T]\}$$

for which $\Re(t) = |I(t)| + |D(t)| + |A(t)| + |P(t)|$. From theorem 2, we know that $I(t)$, $D(t)$, $A(t)$, and $P(t)$ are bounded for all $t \geq 0$, i.e., $\|I(t)\| \leq \eta_1$, $\|D(t)\| \leq \eta_2$, $\|A(t)\| \leq \eta_3$, and $\|P(t)\| \leq \eta_4$, where $\eta_i > 0$ $(i = 1,2,3,4)$ are constants.

Model system (5) can be rewritten as:

$$
\begin{aligned}
{}^{FF-ABC}D_{0,t}^{\alpha,\tau}\{I(t)\} &= \tau t^{\tau-1} F_1(t, I(t)),\\
{}^{FF-ABC}D_{0,t}^{\alpha,\tau}\{D(t)\} &= \tau t^{\tau-1} F_2(t, D(t)),\\
{}^{FF-ABC}D_{0,t}^{\alpha,\tau}\{A(t)\} &= \tau t^{\tau-1} F_3(t, A(t)),\\
{}^{FF-ABC}D_{0,t}^{\alpha,\tau}\{P(t)\} &= \tau t^{\tau-1} F_4(t, P(t)),
\end{aligned}
$$

where

$$
\begin{aligned}
F_1(t,I) &= rI(1 - \frac{I}{K}) - \beta AI - \mu_1 I,\\
F_2(t,D) &= \theta I - \mu_2 AD,\\
F_3(t,A) &= A_0 - \mu_3 A,\\
F_4(t,P) &= P_0 + \delta ID - \gamma AP - \mu_4 P.
\end{aligned}
\tag{6}
$$

With the use of the fractal-fractional integral operator (2) and fixed point theory, we are able to transform the created model system (5) into an integral equation as given below:

$$\begin{cases} I(t) = I(0) + \dfrac{\tau t^{\tau-1}(1-\alpha)}{ABC(\alpha)} F_1(t, I(t)) \\ \qquad + \dfrac{\alpha\tau}{ABC(\alpha)\Gamma(\alpha)} \displaystyle\int_0^t \lambda^{\tau-1}(t-\lambda)^{\alpha-1} F_1(\lambda, I(\lambda))\, d\lambda, \\ D(t) = D(0) + \dfrac{\tau t^{\tau-1}(1-\alpha)}{ABC(\alpha)} F_2(t, D(t)) \\ \qquad + \dfrac{\alpha\tau}{ABC(\alpha)\Gamma(\alpha)} \displaystyle\int_0^t \lambda^{\tau-1}(t-\lambda)^{\alpha-1} F_2(\lambda, D(\lambda))\, d\lambda, \\ A(t) = A(0) + \dfrac{\tau t^{\tau-1}(1-\alpha)}{ABC(\alpha)} F_3(t, A(t)) \\ \qquad + \dfrac{\alpha\tau}{ABC(\alpha)\Gamma(\alpha)} \displaystyle\int_0^t \lambda^{\tau-1}(t-\lambda)^{\alpha-1} F_3(\lambda, A(\lambda))\, d\lambda, \\ P(t) = P(0) + \dfrac{\tau t^{\tau-1}(1-\alpha)}{ABC(\alpha)} F_4(t, P(t)) \\ \qquad + \dfrac{\alpha\tau}{ABC(\alpha)\Gamma(\alpha)} \displaystyle\int_0^t \lambda^{\tau-1}(t-\lambda)^{\alpha-1} F_4(\lambda, P(\lambda))\, d\lambda. \end{cases} \tag{7}$$

Theorem 5. *The kernels $F_1(t,I)$, $F_2(t,D)$, $F_3(t,A)$ and $F_4(t,P)$ satisfy the Lipschitz condition.*

Proof. For any two functions I and I_1, we have

$$\begin{aligned} \|F_1(t,I) - F_1(t,I_1)\| &= \left\| \left[rI\left(1 - \frac{I}{K}\right) - \beta AI - \mu_1 I \right] - \left[rI_1\left(1 - \frac{I_1}{K}\right) - \beta AI_1 - \mu_1 I_1 \right] \right\|, \\ &= \left\| r(I - I_1) - \frac{r}{K}(I^2 - I_1^2) - \beta A(I - I_1) - \mu_1(I - I_1) \right\|, \\ &= \left\| \left(r - \frac{r}{K}(I + I_1) - \beta A - \mu_1 \right)(I - I_1) \right\|, \\ &\leq \left(r + \frac{r}{K}\|I + I_1\| + \beta\|A\| + \mu_1 \right)\|I - I_1\|. \end{aligned}$$

Let $\omega_1 = r + 2\frac{r}{K}\eta_1 + \beta\eta_3 + \mu_1$, then we get

$$\|F_1(t,I) - F_1(t,I_1)\| \leq \omega_1 \|I(t) - I_1(t)\|.$$

Next

$$\begin{aligned} \|F_2(t,D) - F_2(t,D_1)\| &= \|(\theta I - \mu_2 AD) - (\theta I - \mu_2 AD_1)\|, \\ &= \|-\mu_2 A(D - D_1)\|, \\ &\leq \mu_2\|A\|\|D - D_1\|, \\ &\leq \omega_2\|D(t) - D_1(t)\|, \ \ \omega_2 = \mu_2\eta_3. \end{aligned}$$

Again

$$\|F_3(t,A) - F_3(t,A_1)\| = \|(A_0 - \mu_3 A) - (A_0 - \mu_3 A_1)\|,$$

$$\begin{aligned}&= \|-\mu_3(A-A_1)\|,\\ &\leq \omega_3\|A(t)-A_1(t)\|, \quad \omega_3=\mu_3.\end{aligned}$$

Also

$$\begin{aligned}\|F_4(t,P)-F_4(t,P_1)\| &= \|(P_0+\delta ID-\gamma AP-\mu_4 P)-(P_0+\delta ID-\gamma AP_1-\mu_4 P_1)\|,\\ &= \|(-\gamma A-\mu_4)(P-P_1)\|,\\ &\leq (\gamma\|A\|+\mu_4)\|P-P_1\|,\\ &\leq \omega_4\|P(t)-P_1(t)\|, \quad \omega_4=\gamma\eta_3+\mu_4.\end{aligned}$$ □

Theorem 6. *The given FF model (5) has a unique solution if*

$$\Big(\frac{\tau t^{\tau-1}(1-\alpha)}{ABC(\alpha)}+\frac{\alpha\tau\Gamma(\tau)T^{\alpha+\tau-1}}{ABC(\alpha)\Gamma(\alpha+\tau)}\Big)\omega_i<1,\ i\in\{1,2,3,4\}. \tag{8}$$

Proof. Suppose there exists two distinct solutions (I,D,A,P) and (I_1,D_1,A_1,P_1) for model (5). Then using (7), we have

$$\begin{aligned}\|I-I_1\| &= \max_{t\in[0,T]}\Big|\frac{\tau t^{\tau-1}(1-\alpha)}{ABC(\alpha)}\left(F_1(t,I(t))-F_1(t,I_1(t))\right)\\ &\quad+\frac{\alpha\tau}{ABC(\alpha)\Gamma(\alpha)}\int_0^t\lambda^{\tau-1}(t-\lambda)^{\alpha-1}(F_1(\lambda,I(\lambda))-F_1(\lambda,I_1(\lambda)))\,d\lambda\Big|,\\ &\leq \frac{\tau t^{\tau-1}(1-\alpha)}{ABC(\alpha)}\max_{t\in[0,T]}\Big|F_1(t,I(t))-F_1(t,I_1(t))\Big|\\ &\quad+\frac{\alpha\tau}{ABC(\alpha)\Gamma(\alpha)}\max_{t\in[0,T]}\Big|\int_0^1\lambda^{\tau-1}(1-\lambda)^{\alpha-1}t^{\alpha+\tau-1}\big(F_1(\lambda,I(\lambda))-F_1(\lambda,I_1(\lambda))\big)\,d\lambda\Big|,\\ &\leq \frac{\tau t^{\tau-1}(1-\alpha)}{ABC(\alpha)}\|F_1(t,I(t))-F_1(t,I_1(t))\|\\ &\quad+\frac{\alpha\tau\Gamma(\alpha)\Gamma(\tau)T^{\alpha+\tau-1}}{ABC(\alpha)\Gamma(\alpha)\Gamma(\alpha+\tau)}\|F_1(\lambda,I(\lambda))-F_1(\lambda,I_1(\lambda))\|,\\ &\leq \Big(\frac{\tau t^{\tau-1}(1-\alpha)}{ABC(\alpha)}+\frac{\alpha\tau\Gamma(\tau)T^{\alpha+\tau-1}}{ABC(\alpha)\Gamma(\alpha+\tau)}\Big)\omega_1\|I(t)-I_1(t)\|.\end{aligned} \tag{9}$$

Hence

$$0\leq\Big[\Big(\frac{\tau t^{\tau-1}(1-\alpha)}{ABC(\alpha)}+\frac{\alpha\tau\Gamma(\tau)T^{\alpha+\tau-1}}{ABC(\alpha)\Gamma(\alpha+\tau)}\Big)\omega_1-1\Big]\|I(t)-I_1(t)\|.$$

Using relation (8), we have

$$\|I-I_1\|\leq 0,$$

since norm cannot be negative. we get $I=I_1$. Similarly, we can show that

$$0\leq\Big[\Big(\frac{\tau t^{\tau-1}(1-\alpha)}{ABC(\alpha)}+\frac{\alpha\tau\Gamma(\tau)T^{\alpha+\tau-1}}{ABC(\alpha)\Gamma(\alpha+\tau)}\Big)\omega_2-1\Big]\|D(t)-D_1(t)\|,$$

$$0 \leq \Big[\Big(\frac{\tau t^{\tau-1}(1-\alpha)}{ABC(\alpha)} + \frac{\alpha\tau\Gamma(\tau)T^{\alpha+\tau-1}}{ABC(\alpha)\Gamma(\alpha+\tau)}\Big)\omega_3 - 1\Big]\|A(t) - A_1(t)\|,$$
$$0 \leq \Big[\Big(\frac{\tau t^{\tau-1}(1-\alpha)}{ABC(\alpha)} + \frac{\alpha\tau\Gamma(\tau)T^{\alpha+\tau-1}}{ABC(\alpha)\Gamma(\alpha+\tau)}\Big)\omega_4 - 1\Big]\|P(t) - P_1(t)\|.$$

Thus, $D = D_1$, $A = A_1$ and $P = P_1$. So, the FF model (5) has a unique solution when the relation (8) holds. □

9 Stability analysis

Stability is a fundamental aspect of differential equations, with Lyapunov, exponential, and asymptotic types commonly studied. Ulam–Hyers stability is especially important for optimization and numerical analysis, as it provides a link between exact solutions and their numerical approximations. While Lyapunov stability examines the sensitivity of exact trajectories to initial perturbations, Ulam–Hyers stability ensures that any approximate solution-such as those obtained numerically or experimentally-remains close to an exact solution. This is particularly valuable for FF models with nonlocal memory effects, where analytical solutions are often unavailable. Establishing Ulam–Hyers stability therefore confirms the robustness and reliability of the model under small perturbations, making it directly relevant for real-world applications and numerical simulations.

Following the approaches presented in [25, 26], Ulam–Hyers stability is analyzed in this section.

Definition 3. *For model (5) to have Ulam–Hyers stability, the following conditions must meet for every constant $\xi_i > 0$, $i \in \mathbb{N}^4$:*

$$\left|I(t) - \frac{\tau t^{\tau-1}(1-\alpha)}{ABC(\alpha)}F_1(t,I(t)) - \frac{\alpha\tau}{ABC(\alpha)\Gamma(\alpha)}\int_0^t \lambda^{\tau-1}(t-\lambda)^{\alpha-1}F_1(\lambda,I(\lambda))\,d\lambda\right| \leq \xi_1,$$
$$\left|D(t) - \frac{\tau t^{\tau-1}(1-\alpha)}{ABC(\alpha)}F_2(t,D(t)) - \frac{\alpha\tau}{ABC(\alpha)\Gamma(\alpha)}\int_0^t \lambda^{\tau-1}(t-\lambda)^{\alpha-1}F_2(\lambda,D(\lambda))\,d\lambda\right| \leq \xi_2,$$
$$\left|A(t) - \frac{\tau t^{\tau-1}(1-\alpha)}{ABC(\alpha)}F_3(t,A(t)) - \frac{\alpha\tau}{ABC(\alpha)\Gamma(\alpha)}\int_0^t \lambda^{\tau-1}(t-\lambda)^{\alpha-1}F_3(\lambda,A(\lambda))\,d\lambda\right| \leq \xi_3,$$
$$\left|P(t) - \frac{\tau t^{\tau-1}(1-\alpha)}{ABC(\alpha)}F_4(t,P(t)) - \frac{\alpha\tau}{ABC(\alpha)\Gamma(\alpha)}\int_0^t \lambda^{\tau-1}(t-\lambda)^{\alpha-1}F_4(\lambda,P(\lambda))\,d\lambda\right| \leq \xi_4.$$

For model (5), there is an approximation $\Big(I_1(t), D_1(t), A_1(t), P_1(t)\Big)$ that satisfies the following integral equations:

$$I_1(t) = \frac{\tau t^{\tau-1}(1-\alpha)}{ABC(\alpha)}F_1(t,I_1(t)) + \frac{\alpha\tau}{ABC(\alpha)\Gamma(\alpha)}\int_0^t \lambda^{\tau-1}(t-\lambda)^{\alpha-1}F_1(\lambda,I_1(\lambda))\,d\lambda,$$
$$D_1(t) = \frac{\tau t^{\tau-1}(1-\alpha)}{ABC(\alpha)}F_2(t,D_1(t)) + \frac{\alpha\tau}{ABC(\alpha)\Gamma(\alpha)}\int_0^t \lambda^{\tau-1}(t-\lambda)^{\alpha-1}F_2(\lambda,D_1(\lambda))\,d\lambda,$$
$$A_1(t) = \frac{\tau t^{\tau-1}(1-\alpha)}{ABC(\alpha)}F_3(t,A_1(t)) + \frac{\alpha\tau}{ABC(\alpha)\Gamma(\alpha)}\int_0^t \lambda^{\tau-1}(t-\lambda)^{\alpha-1}F_3(\lambda,A_1(\lambda))\,d\lambda,$$
$$P_1(t) = \frac{\tau t^{\tau-1}(1-\alpha)}{ABC(\alpha)}F_4(t,P_1(t)) + \frac{\alpha\tau}{ABC(\alpha)\Gamma(\alpha)}\int_0^t \lambda^{\tau-1}(t-\lambda)^{\alpha-1}F_4(\lambda,P_1(\lambda))\,d\lambda,$$

so that

$$\begin{aligned} |I-I_1| &\le \nu_1\omega_1, \\ |D-D_1| &\le \nu_2\omega_2, \\ |A-A_1| &\le \nu_3\omega_3, \\ |P-P_1| &\le \nu_4\omega_4. \end{aligned} \tag{10}$$

Theorem 7. *If (10) holds, then model problem (5) is Ulam–Hyers stable.*

Proof. We have

$$\begin{aligned} |I-I_1| &= \Big| \frac{\tau t^{\tau-1}(1-\alpha)}{ABC(\alpha)} \left(F_1(t,I(t)) - F_1(t,I_1(t))\right) \\ &\quad + \frac{\alpha\tau}{ABC(\alpha)\Gamma(\alpha)} \int_0^t \lambda^{\tau-1}(t-\lambda)^{\alpha-1}\left(F_1(\lambda,I(\lambda)) - F_1(\lambda,I_1(\lambda))\right) d\lambda \Big|, \\ &\le \max_{t\in[0,T]} \Big| \frac{\tau t^{\tau-1}(1-\alpha)}{ABC(\alpha)} \left(F_1(t,I(t)) - F_1(t,I_1(t))\right) \\ &\quad + \frac{\alpha\tau}{ABC(\alpha)\Gamma(\alpha)} \int_0^t \lambda^{\tau-1}(t-\lambda)^{\alpha-1}\left(F_1(\lambda,I(\lambda)) - F_1(\lambda,I_1(\lambda))\right) d\lambda \Big|, \\ &\le \Big(\frac{\tau t^{\tau-1}(1-\alpha)}{ABC(\alpha)} + \frac{\alpha\tau\Gamma(\tau)T^{\alpha+\tau-1}}{ABC(\alpha)\Gamma(\alpha+\tau)} \Big) \omega_1 \|I-I_1\|, \quad \text{(using Eq. (9))}. \end{aligned}$$

Then

$$|I-I_1| \le \nu_1\omega_1, \quad \text{with} \quad \nu_1 = \Big(\frac{\tau t^{\tau-1}(1-\alpha)}{ABC(\alpha)} + \frac{\alpha\tau\Gamma(\tau)T^{\alpha+\tau-1}}{ABC(\alpha)\Gamma(\alpha+\tau)} \Big) \|I-I_1\|.$$

Similarly, we can obtain

$$\begin{aligned} |D-D_1| &\le \nu_2\omega_2, \quad \text{with} \quad \nu_2 = \Big(\frac{\tau t^{\tau-1}(1-\alpha)}{ABC(\alpha)} + \frac{\alpha\tau\Gamma(\tau)T^{\alpha+\tau-1}}{ABC(\alpha)\Gamma(\alpha+\tau)} \Big) \|D-D_1\|, \\ |A-A_1| &\le \nu_3\omega_3, \quad \text{with} \quad \nu_3 = \Big(\frac{\tau t^{\tau-1}(1-\alpha)}{ABC(\alpha)} + \frac{\alpha\tau\Gamma(\tau)T^{\alpha+\tau-1}}{ABC(\alpha)\Gamma(\alpha+\tau)} \Big) \|A-A_1\|, \\ |P-P_1| &\le \nu_4\omega_4, \quad \text{with} \quad \nu_4 = \Big(\frac{\tau t^{\tau-1}(1-\alpha)}{ABC(\alpha)} + \frac{\alpha\tau\Gamma(\tau)T^{\alpha+\tau-1}}{ABC(\alpha)\Gamma(\alpha+\tau)} \Big) \|P-P_1\|. \end{aligned}$$

Hence, the results follows. □

10 Sensitivity analysis

In this section, we analyze the sensitivity for some of the parameters utilized in the system under consideration. The parameters that significantly affect the threshold quantity are found using the assistance approach. The sensitivity index of $\mathfrak{R}_\circ$ is computed using Chintis's method [6]. Particularly, the following formula gives the sensitivity index $\Delta_b^{\mathfrak{R}_\circ}$ of a parameter b:

$$\Delta_b^{\mathfrak{R}_\circ} = \frac{\partial \mathfrak{R}_\circ}{\partial b} \frac{b}{\mathfrak{R}_\circ}.$$

Table 2: Sensitivity indices of $\mathfrak{R}_o$ in relation to the model's parameters

Sensitivity index	Value
$\Delta_r^{\mathfrak{R}_o}$	1
$\Delta_\beta^{\mathfrak{R}_o}$	-0.99
$\Delta_{\mu_1}^{\mathfrak{R}_o}$	-0.0074
$\Delta_{A_0}^{\mathfrak{R}_o}$	-0.99
$\Delta_{\mu_3}^{\mathfrak{R}_o}$	11.028

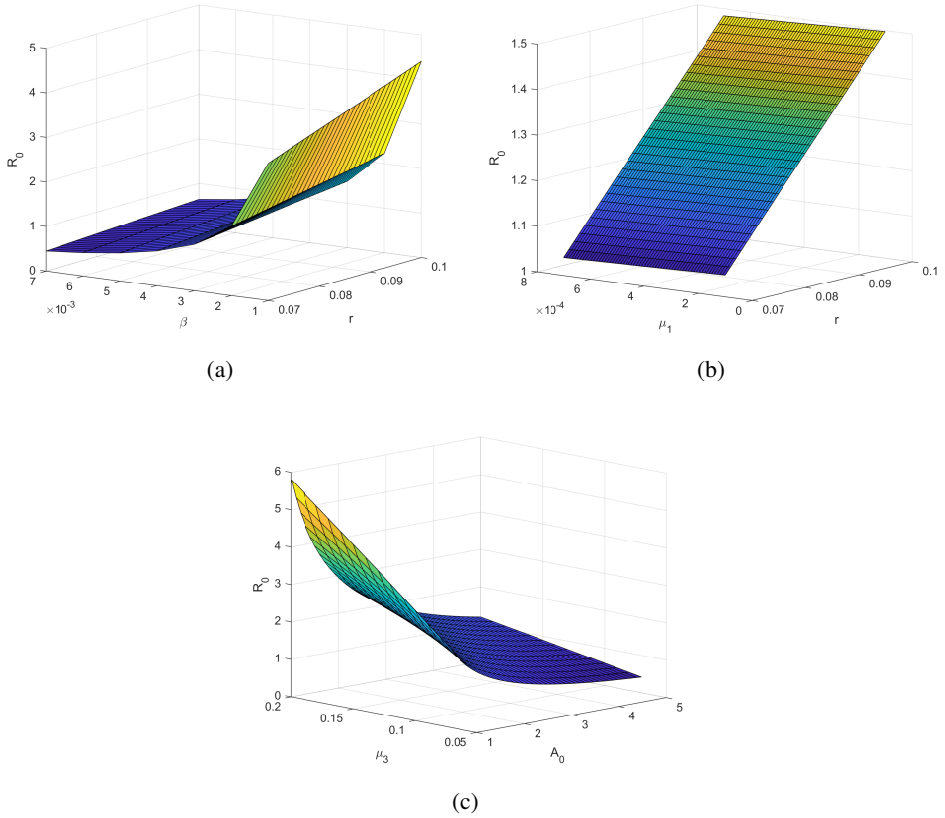

Figure 1: Sensitivity analysis plot for threshold number $\mathfrak{R}_o$ with different parameters

The sensitivity indices for the various parameters in the suggested model are shown in Table 2. A positive sensitivity index indicates a direct proportional relationship between $\mathfrak{R}_o$ and the corresponding parameters, while a negative index signifies an inverse proportional relationship.

The results of the sensitivity analysis indicate that the threshold number $\mathfrak{R}_o$ is most sensitive to changes in the parameters r and μ_3, as depicted in Figures 1(a)–(c). Changes in these parameters, whether increasing or decreasing, have a proportional impact on $\mathfrak{R}_o$. Specifically, an increase in industrialization (r) leads to escalating deforestation and pollution. On the other hand, if any one of the three parameters

increases, $\mathfrak{R}_o$ will decreases. Note that A_0 represents the afforestation growth rate. From the figure 1(c), we can conclude that increasing afforestation is essential to mitigate the deforestation and pollution resulting from industrialization.

11 Numerical scheme for FF operator

The generalized Adams–Bashforth method with Lagrange interpolation [3, 4], formulated for the fractal–fractional derivative in the sense of Atangana–Baleanu, is employed to evaluate and predict the numerical stability of the established model (5). The numerical scheme for our FF model is given as follows:

$$
\begin{aligned}
I(t_{n+1}) &= I(t_0) + \frac{\tau t_n^{\tau-1}(1-\alpha)}{ABC(\alpha)} F_1(t_n, I(t_n)) + \frac{\tau(\Delta t)^\alpha}{ABC(\alpha)\Gamma(\alpha+2)} \sum_{k=0}^{n} \Big[t_k^{\tau-1} F_1(t_k, I(t_k)) \\
&\quad \Big((n+1-k)^\alpha (n-k+2+\alpha) - (n-k)^\alpha (n-k+2+2\alpha) \Big) \\
&\quad - t_{k-1}^{\tau-1} F_1(t_{k-1}, I(t_{k-1})) \Big((n+1-k)^{\alpha+1} - (n-k)^\alpha (n-k+1+\alpha) \Big) \Big], \\
D(t_{n+1}) &= D(t_0) + \frac{\tau t_n^{\tau-1}(1-\alpha)}{ABC(\alpha)} F_2(t_n, D(t_n)) + \frac{\tau(\Delta t)^\alpha}{ABC(\alpha)\Gamma(\alpha+2)} \sum_{k=0}^{n} \Big[t_k^{\tau-1} F_2(t_k, D(t_k)) \\
&\quad \Big((n+1-k)^\alpha (n-k+2+\alpha) - (n-k)^\alpha (n-k+2+2\alpha) \Big) \\
&\quad - t_{k-1}^{\tau-1} F_2(t_{k-1}, D(t_{k-1})) \Big((n+1-k)^{\alpha+1} - (n-k)^\alpha (n-k+1+\alpha) \Big) \Big], \\
A(t_{n+1}) &= A(t_0) + \frac{\tau t_n^{\tau-1}(1-\alpha)}{ABC(\alpha)} F_3(t_n, A(t_n)) + \frac{\tau(\Delta t)^\alpha}{ABC(\alpha)\Gamma(\alpha+2)} \sum_{k=0}^{n} \Big[t_k^{\tau-1} F_3(t_k, A(t_k)) \\
&\quad \Big((n+1-k)^\alpha (n-k+2+\alpha) - (n-k)^\alpha (n-k+2+2\alpha) \Big) \\
&\quad - t_{k-1}^{\tau-1} F_3(t_{k-1}, A(t_{k-1})) \Big((n+1-k)^{\alpha+1} - (n-k)^\alpha (n-k+1+\alpha) \Big) \Big], \\
P(t_{n+1}) &= P(t_0) + \frac{\tau t_n^{\tau-1}(1-\alpha)}{ABC(\alpha)} F_4(t_n, P(t_n)) + \frac{\tau(\Delta t)^\alpha}{ABC(\alpha)\Gamma(\alpha+2)} \sum_{k=0}^{n} \Big[t_k^{\tau-1} F_4(t_k, P(t_k)) \\
&\quad \Big((n+1-k)^\alpha (n-k+2+\alpha) - (n-k)^\alpha (n-k+2+2\alpha) \Big) \\
&\quad - t_{k-1}^{\tau-1} F_4(t_{k-1}, P(t_{k-1})) \Big((n+1-k)^{\alpha+1} - (n-k)^\alpha (n-k+1+\alpha) \Big) \Big].
\end{aligned}
$$

12 Numerical simulation and discussion

In this section, we conduct a numerical simulation to the FF system (5) using the method presented in the previous section. For the numerical experiment, the initial conditions are chosen as $(23, 20, 25, 10)$ and the set of parameter values $r = 0.09$, $K = 100$, $\beta = 0.003$, $\mu_1 = 0.0005$, $\theta = 0.07$, $\mu_2 = 0.004$, $A_0 = 3$, $\mu_3 = 0.09$, $\delta = 0.001$, $\gamma = 0.002$, $P_0 = 7$, $\mu_4 = 0.008$. Based on these initial values and parameters, the equilibrium point is $E^0 = (0, 0, 33.34, 93.75)$, which is found to be locally asymptotically stable. The corresponding time-series trajectories of the system variables are depicted in Figures 2(a)-(d)

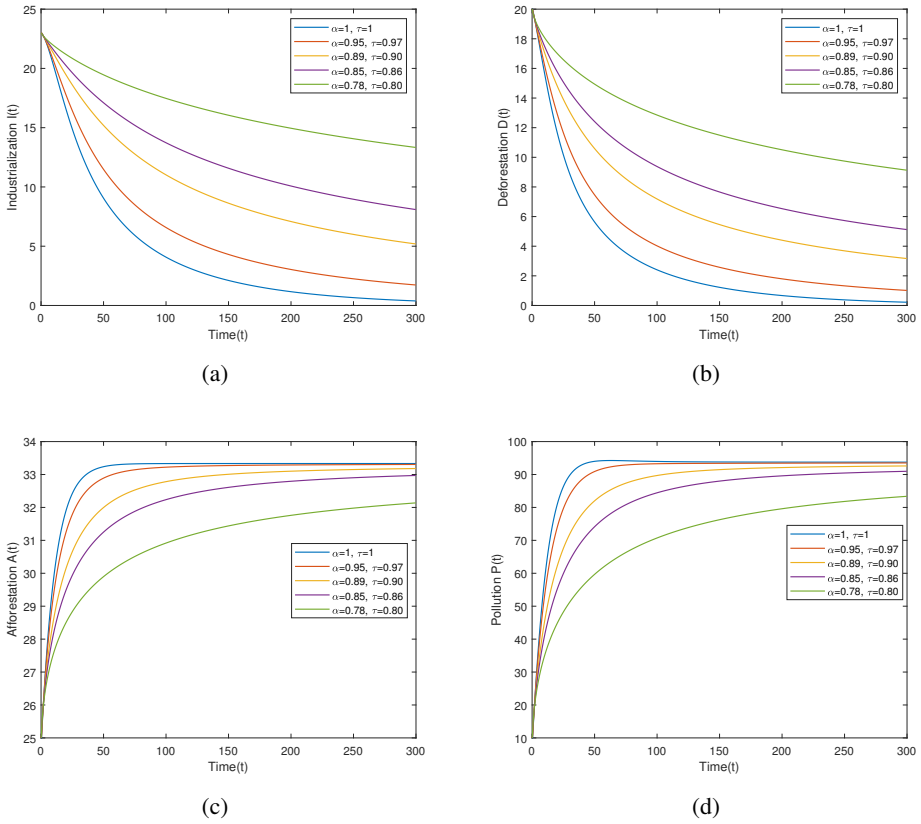

Figure 2: Time series solution of (a) Level of industrialization, (b) Level of deforestation, (c) Level of afforestation, and (d) Level of pollution for different values of α, τ when $\mathfrak{R}_o < 1$

for $\mathfrak{R}_o = 0.8955 < 1$ under various combinations of fractional and fractal orders: (i) $\alpha = 1, \tau = 1$, (ii) $\alpha = 0.95, \tau = 0.97$, (iii) $\alpha = 0.89, \tau = 0.90$, (iv) $\alpha = 0.85, \tau = 0.86$, (v) $\alpha = 0.78, \tau = 0.80$. In each case, the system trajectories converge toward the equilibrium point E^0, confirming the local stability of the steady state when $\mathfrak{R}_o < 1$. This outcome demonstrates that maintaining $\mathfrak{R}_o$ below unity is crucial for minimizing deforestation and pollution associated with industrial expansion. When the threshold parameter $\mathfrak{R}_o$ is less than one, the intrinsic growth rate of industrialization becomes inadequate to overcome the effects of afforestation and regulatory control. As a result, industrial activity declines over time. Furthermore, as the fractional order α approaches unity, the system gradually loses its memory property, and its dynamics approach those of an integer-order system, which reacts more swiftly to current changes and depends less on historical states. Under this regime, the decrease in industrialization reduces deforestation, while afforestation increases due to the lowered anthropogenic impact. Conversely, pollution levels exhibit an upward trend because the reduced memory effect weakens the system's cumulative environmental recovery capacity, allowing pollutants to build up more rapidly than they dissipate. Environmentally, this implies that although industrial and deforestation pressures can be effectively managed in a less memory-dependent system, pollution may continue to rise owing to the persistent influence of previously accumulated contaminants.

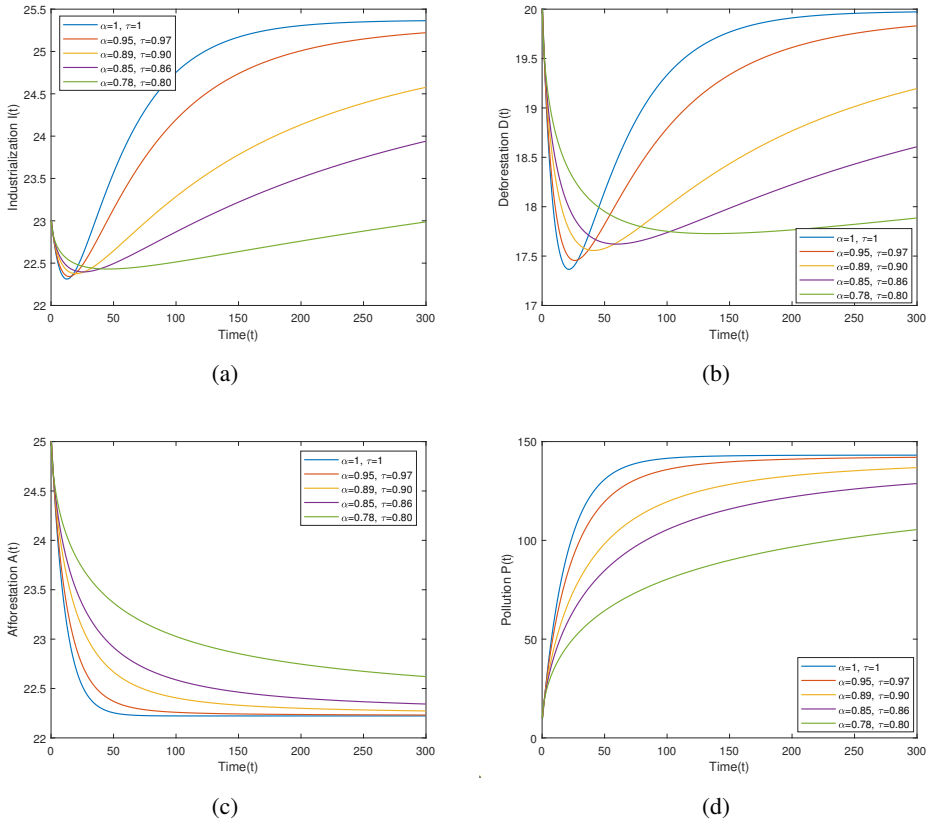

Figure 3: Time series solution of (a) Level of industrialization, (b) Level of deforestation, (c) Level of afforestation, and (d) Level of pollution for different values of α, τ when $\mathfrak{R}_o > 1$

By changing the parameter value to $A_0 = 2$ while keeping the other parameters fixed, the system admits a coexisting equilibrium point $E^* = (25.37, 19.98, 22.22, 143.14)$, which is found to be locally asymptotically stable for $\mathfrak{R}_o = 1.34 > 1$. The corresponding time-series trajectories of the system variables are illustrated in Figures 3(a)-(d) for the fractional–fractal order combinations: (i) $\alpha = 1, \tau = 1$, (ii) $\alpha = 0.95, \tau = 0.97$, (iii) $\alpha = 0.89, \tau = 0.90$, (iv) $\alpha = 0.85, \tau = 0.86$, (v) $\alpha = 0.78, \tau = 0.80$. As expected, the solutions of system (5) converge toward the equilibrium point E^*, confirming the system's stability. When the threshold parameter $\mathfrak{R}_o$ exceeds unity, the rate of industrial growth outweighs the combined effects of afforestation and regulatory control, promoting a self-sustaining expansion of industrialization. As the fractional order approaches unity, the system gradually loses its memory property, leading the dynamics to behave more like those of a classical integer-order model with faster responses to current conditions and reduced influence from historical states. Consequently, industrialization intensifies, accompanied by an increase in deforestation and a decline in afforestation activities. The escalation of industrial and deforestation processes elevates pollution levels due to greater emissions and the weakening of environmental memory, which diminishes the system's capacity for natural recovery. This regime characterizes a high-growth yet ecologically unstable state, where rapid industrial advancement drives deforestation and pollution, ultimately compromising environmental sustainability.

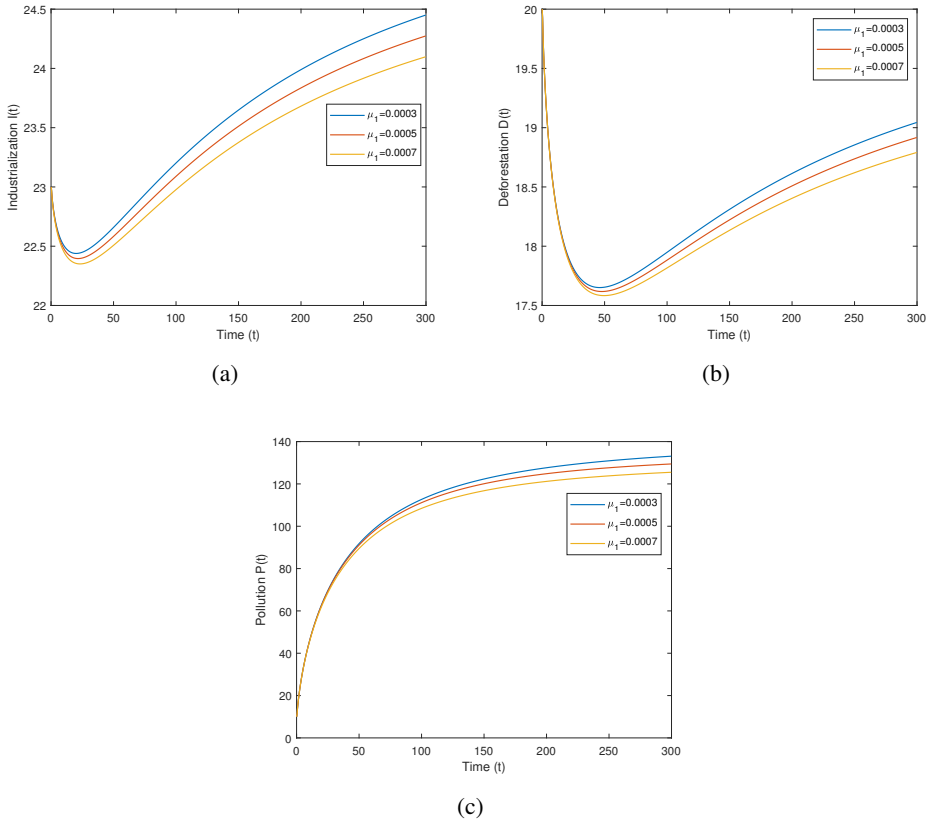

Figure 4: Effects of parameter μ_1 on (a) Level of industrialization, (b) Level of deforestation, and (c) Level of pollution for $\alpha = 0.85, \tau = 0.90$

For $\alpha = 0.85$ and $\tau = 0.90$, Figures 4(a)-(c) illustrate the influence of the control parameter μ_1, representing government regulation on industrialization. As μ_1 increases, the intensity of industrial activities declines due to stricter enforcement of environmental policies and technological restrictions. This reduction in industrialization leads to a corresponding decrease in deforestation and pollution levels. Physically, this behavior implies that effective government interventions-such as emission limits, industrial zoning, or reforestation mandates-can significantly mitigate the environmental impacts of industrial growth. Hence, strengthening regulatory measures plays a crucial role in maintaining ecological balance by controlling excessive industrial expansion and promoting sustainable resource management.

For $\alpha = 0.85$ and $\tau = 0.90$, Figures 5(a)-(d) illustrate the impact of increasing A_0, the rate of afforestation, on the system's behavior. As A_0 rises, forest regeneration intensifies, enhancing the natural capacity of the environment to absorb carbon dioxide and other pollutants. This leads to a gradual decline in both pollution and deforestation levels, even under continuing industrial influence. Physically, this reflects how sustained afforestation initiatives-such as replanting degraded lands, expanding green cover, and conserving existing forests-an mitigate the adverse effects of industrialization. The increased vegetation cover not only supports biodiversity and soil stability but also serves as a long-term buffer against environmental degradation, promoting ecological resilience and sustainability.

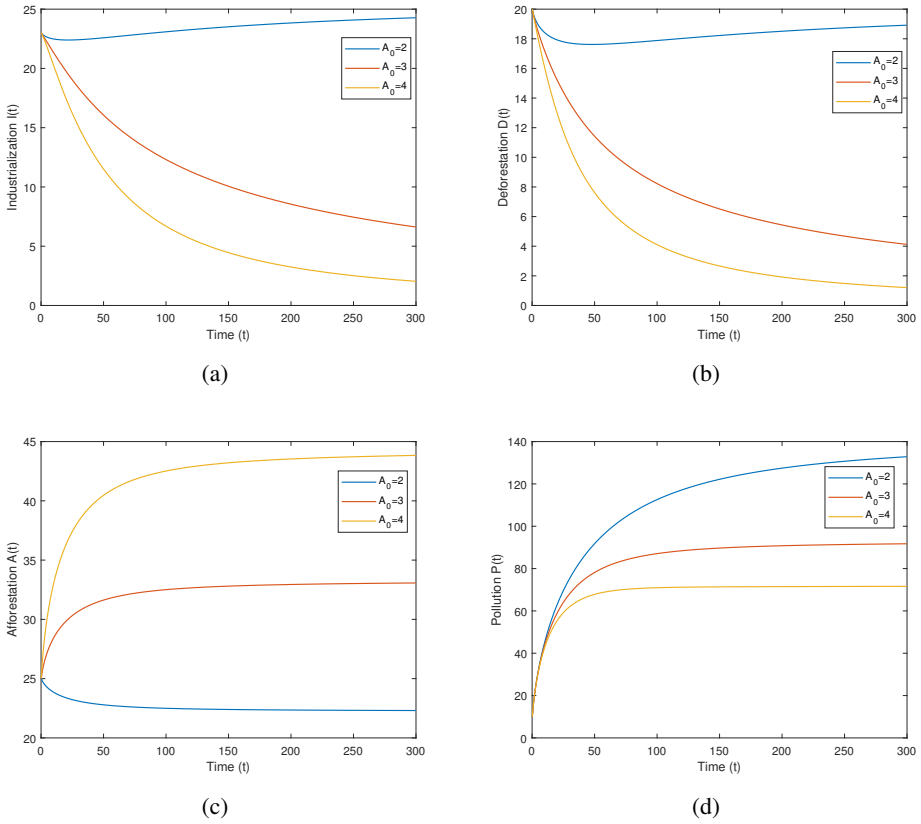

Figure 5: Effects of parameter A_0 on (a) Level of industrialization, (b) Level of deforestation, (c) Level of afforestation, and (d) Level of pollution for $\alpha = 0.85, \tau = 0.90$

13 Conclusion

In this study, we developed a fractal–fractional mathematical model to investigate the impact of industrialization on deforestation and environmental pollution. Starting with a classical integer-order formulation, we extended the model using the Atangana–Baleanu–Caputo Fractal-Fractional operator with a generalized Mittag-Leffler kernel. We investigated the existence and stability of solutions, conducted a comparative study across different fractal-fractional orders, and demonstrated the local asymptotic stability of equilibrium points. Using non-linear functional analysis, we established Ulam–Hyers stability and identified key parameters through sensitivity analysis. Numerical simulations with Lagrange interpolation confirmed the precision of the stability analysis, with graphical results highlighting the model's effectiveness in capturing pollution dynamics. The graphical results indicate that the fractal-fractional model offers deeper insights into dynamics of complex systems and can be reliably utilized as an effective modeling tool. Future work could include stochastic effects, integration with socio-economic factors, and validation with real-world data. Exploring higher-order fractal–fractional operators and implementing optimization or control strategies would further enhance the model's applicability for sustainable development planning.

Conflict of interest

The authors declare that they have no conflict of interest.

References

[1] A. Atangana, *Fractal-fractional differentiation and integration: connecting fractal calculus and fractional calculus to predict complex system*, Chaos Solitons Fract. **102** (2017) 396–406.

[2] A. Atangana, D. Baleanu, *New fractional derivatives with nonlocal and non-singular kernel: theory and application to heat transfer model*, (2016) arXiv preprint arXiv:1602.03408 .

[3] A. Atangana, S. Qureshi, *Modeling attractors of chaotic dynamical systems with fractal–fractional operators*, Chaos Solitons Fract. **123** (2019) 320–337.

[4] M. Awadalla, M. Rahman, F.S. Al-Duais, A. Al-Bossly, K. Abuasbeh, M. Arab, *Exploring the role of fractal-fractional operators in mathematical modelling of corruption*, Appl. Math. Sci. Eng. **31** (2023) 2233678.

[5] M. Caputo, M. Fabrizio, *A new definition of fractional derivative without singular kernel*, Prog. Fract. Differ. Appl. **1** (2015) 73–85.

[6] N. Chitnis, J.M. Cushing, J.M. Hyman, *Bifurcation analysis of a mathematical model for malaria transmission*, SIAM J. Appl. Math. **67** (2006) 24–45.

[7] B. Dubey, B. Das, *Models for the survival of species dependent on resource in industrial environments*, J. Math. Anal. Appl. **231** (1999) 374–396.

[8] S. Etemad, I. Avci, P. Kumar, D. Baleanu, S. Rezapour, *Some novel mathematical analysis on the fractal–fractional model of the AH1N1/09 virus and its generalized Caputo-type version*, Chaos Solitons Fract. **162** (2022) 112511.

[9] M. Fahimi, K. Nouri, L. Torkzadeh, *Analytical investigation of fractional SEIRVQD measles mathematical model*, J. Math. Model. **13** (2025) 393–413.

[10] J.F. Gomez-Aguilar, T. Cordova-Fraga, T. Abdeljawad, A. Khan, H. Khan, *Analysis of fractal-fractional malaria transmission model*, Fractals **28** (2020) 2040041.

[11] K. Jyotsna, A. Tandon, *A mathematical model to study the impact of mining activities and pollution on forest resources and wildlife population*, J. Biol. Syst. **25** (2017) 207–230.

[12] S. Karthikeyan, P. Ramesh, M. Sambath, *Stability analysis of fractional-order predator-prey model with anti-predator behaviour and prey refuge*, J. Math. Model. **11(3)** (2023) 527–546.

[13] H. Khan, J. Alzabut, A. Shah, Z.Y. He, S. Etemad, S. Rezapour, A. Zada, *On fractal-fractional waterborne disease model: A study on theoretical and numerical aspects of solutions via simulations*, Fractals **31** (2023) 2340055.

[14] X. Liu, S. Ahmad, M. Rahman, Y. Nadeem, A. Akgul, *Analysis of a TB and HIV co-infection model under Mittag-Leffler fractal-fractional derivative*, Phys. Scr. **97** (2022) 054011.

[15] N. Madani, Z. Hammouch, E. H. Azroul, *New model of HIV/AIDS dynamics based on Caputo–Fabrizio derivative order: Optimal strategies to control the spread*, J. Comput. Sci. **90** (2025) 102612.

[16] T. Mekkaoui, Z. Hammouch, *Approximate analytical solutions to the Bagley-Torvik equation by the fractional iteration method*, Ann. Univ. Craiova Math. Comput. Sci. Ser. **39** (2012) 251–256.

[17] A.K. Misra, K. Lata, J.B. Shukla, *A mathematical model for the depletion of forestry resources due to population and population pressure augmented industrialization*, Int. J. Model. Simul. Sci. Comput. **5** (2014) 1350022.

[18] I. Podlubny, *Fractional Differential Equations: An Introduction to Fractional Derivatives, Ffractional Differential Equations, to Methods of their Solution and Some of their Applications*, Elsevier, 1998.

[19] M. Rahman, *Generalized fractal–fractional order problems under non-singular Mittag-Leffler kernel*, Results Phys. **35** (2022) 105346.

[20] K. Shah, M. Arfan, I. Mahariq, A. Ahmadian, S. Salahshour, M. Ferrara, *Fractal-fractional mathematical model addressing the situation of corona virus in Pakistan*, Results Phys. **19** (2020) 103560.

[21] J.B. Shukla, B. Dubey, *Modelling the depletion and conservation of forestry resources: effects of population and pollution*, J. Math. Biol. **36** (1997) 71–94.

[22] J.B. Shukla, H.I. Freedman, V.M. Pal, O.P. Misra, M. Agarwal, A. Shukla, *Degradation and subsequent regeneration of a forestry resource: a mathematical model*, Ecol. Model. **44** (1989) 219–229.

[23] A. Singh, S. Pippal, J. Sati, *Atangana–Baleanu–Caputo (ABC), Caputo-Fabrizio (CF), and Caputo fractional derivative approaches in fuzzy time fractional cancer tumor growth models*, J. Math. Model. **13(3)** (2025) 685–706.

[24] M.F. Uddin, M G. Hafez, Z. Hammouch, H. Rezazadeh, B. Baleanu, *Traveling wave with beta derivative spatial-temporal evolution for describing the nonlinear directional couplers with metamaterials via two distinct methods*, Alex. Eng. J. **60** (2021) 1055–1065.

[25] S.M. Ulam, *A Collection of Mathematical Problems*, Interscience Publishers, 1960.

[26] S.M. Ulam, *Problems in Modern Mathematics*, Courier Corporation, 2004.

[27] L. Verma, R. Meher, D.P. Pandya, *Parameter estimation study of temporal fractional HIV/AIDS transmission model with fractal dimensions using real data in India*, Math. Comput. Simul. **234** (2025) 135–150.

[28] L. Verma, R. Meher, *Study on generalized fuzzy fractional human liver model with Atangana–Baleanu–Caputo fractional derivative*, Eur. Phys. J. Plus **137** (2022) 1233.

[29] L. Verma, R. Meher, O. Nikan, A.A. Al-Saedi, *Numerical study on fractional order nonlinear SIR-SI model for dengue fever epidemics*, Sci. Rep. **15** (2022) 30677.

[30] M.A.U. Waqih, N.A. Bhutto, N.H. Ghumro, S. Kumar, M.A. Salam, *Rising environmental degradation and impact of foreign direct investment: an empirical evidence from SAARC region*, J. Environ. Manag. **243** (2019) 472–480.